Virtual Time-response based Iterative Gain Evaluation and Redesign

Mato Kosaka [*] **Ayato Kosaka** [**] **Manabu Kosaka** [***]

[*] *Information science, Nara Institute of Science and Technology (NAIST); 8916-5 Takayamacho Ikoma JAPAN (e-mail: taba.kosaka@gmail.com).*
[**] *College of Science and Engineering, Aoyama Gakuin University; 5-10-1 Fuchinobe, Chuo-ku, Sagamihara JAPAN (e-mail: kosaka_ayato@yahoo.co.jp)*
[***] *Faculty of Science and Engineering, Kinki University; 3-4-1 Kowakae Higashiosaka JAPAN (e-mail: kosaka@mech.kindai.ac.jp)*

Abstract: Since Artificial Intelligence (AI) has won over human pros such as Chess, Shogi and Go, expectations for AI have been increasing dramatically. One of the reasons why AI has developed so much is the tremendous increase in the processing speed of computers, which makes it possible to virtually repeat simulated competitions such as Othello, Shogi, Go and so on in the computer very fast. Finally, AI has gained strength over human pros. Also in control engineering, if gain tuning experiments of controllers can be virtually performed in a computer, it can be expected to dramatically improve control performance with an AI-like approach. This paper proposes a new method called 'Virtual Time-response based Iterative Gain Evaluation and Redesign' (V-Tiger) which iterates: 1) to calculate virtual time responses of the closed-loop system when a certain controller is inserted based on one-shot experimental data, 2) to measure the overshoot and settling time from the virtual time responses, and 3) to evaluate and redesign the controller gain considering the stability margin.

Keywords: Data-driven control, Time-response, Stability margin, Frequency-response, Virtual reference feedback tuning.

1. INTRODUCTION

Since Artificial Intelligence (AI) has won over human pros such as Chess, Shogi and Go, expectations for AI have been increasing dramatically, see [Silver et al. (2017)]. One of the reasons why AI has developed so much is the tremendous increase in the processing speed of computers, which makes it possible to virtually repeat simulated competitions such as Othello, Shogi, Go and so on in the computer very fast. Finally, AI has gained strength over human pros.

Also in control engineering, if controller gain tuning experiments can be virtually performed in a computer, it can be expected to dramatically improve control performance with the AI-like approach. The tuning experiments often evaluate settling time and overshoot that can be measured from the time response, see [Mnih et al. (2015), Sample (2017), and MATLAB (2010)]. The time response can be accurately calculated by simulation if an accurate model of the controlled object is obtained. For example, the controller tuning of an inverted cart-pole using reinforcement learning in [Mnih et al. (2015) and Surma (2017)], and MATLAB's PIDtune [MATLAB (2010)] optimizes the controller by repeatedly simulating and evaluating the time response based on the model. However, there are two problems with such a model-based AI-like approach. One is that in reinforcement learning, the neural network type controller is black-boxed and the stability of the system cannot be analyzed. Second, it must be a system that can be completely simulated by a computer, see [Sample (2017)]. Chess, Shogi, Go, etc. which AI has dealt with can be completely simulated in a computer because they follow regular rules. However, it is impossible to imitate completely the actual controlled objects including motors, robots, and plants these are handled by control engineering. Therefore, the following approach called model-based control is mainstream in control engineering.

1) Using the experimental data, an accurate model of the controlled object is obtained by system identification.
2) In order to avoid instability of the system due to deviation (uncertainty or noise) between the obtained model and the actual controlled object, the controller is designed in consideration of the closed-loop pole, stability margin, sensitivity, model matching, etc..
3) The time responses in the actual machine experiment are evaluated, and if the desired time response of the closed-loop system is not obtained, it is done again from design 2) or identification 1).

However, when it is necessary to repeat the experiment many times, there is a problem that it is time-consuming and labor-intensive.

To solve the above problems, a method with the following three features are desired: 1) The controller is not black box but linear, 2) It is not necessary to obtain a mathematical model by system identification, and 3) The time response of the closed-loop system can be evaluated in addition to the stability margin at the design stage. In this study, we propose a new method with these three features, Virtual Time-response based Iterative Gain Evaluation and Redesign (V-Tiger). The feature of this method is that the frequency response of the feedback system is obtained from the Fourier transform of the experimental data and the frequency characteristics of the controller, and the virtual time response is obtained by the inverse Fourier transform.

From here, we will discuss the related research and the positioning of this research. A new approach to predict the responses in closed-loop systems based on the direct usage of one-shot experimental data has been proposed in [Kaneko et al. (2019)], but there is a problem that the structure (the numerator and denominator orders of the transfer function) was known because this was required to identify the closed-loop system transfer function model. Since our method does not require identification, there is no such problem. Data-driven control that designs controllers with one-shot experimental data without model identification has been studied. Most of them are based on model-matching to a reference model (transfer function from reference input to output response) in the time domain, see [Campi et al. (2002) and Kaneko et al. (2004)], but there is a problem that the system becomes unstable depending on the reference model, see [Campi et al. (2002) and Yamamoto (2009)]. Since our method does not require a reference model, there is no such problem. There are data-driven control methods designed in the frequency domain in [Steinbuch et al. (2015) and Karimi et al. (2015)], but the time responses are not evaluated. There is a design method that evaluates settling time in [Ohta et al. (2018)], but it is limited to controlled objects that can be approximated as a second-order lag system. Our method has no limitation on the order of the controlled object. This paper organized as follows: Section 2 describes the proposed method, and Section 3 and 4 verify the usefulness of our method by numerical simulation and actual experiments.

2. PROPOSED METHOD

2.1 Calculation of virtual time response of the closed-loop system

The step response (for example, the waveform in Fig. 1a) is a transient response and is able to be calculated using a transfer function model based on the Laplace transform. Also, when a periodic pulse that repeats 1 and 0 at a constant period is input, if the period is long enough, it becomes a periodic response that repeats the step response (for example, the waveform of Fig. 1b), and then its frequency components can be accurately calculated by Fourier transformation. Therefore, we came up with an idea that, by combining the calculated frequency components of the input and output of the controlled object with the frequency characteristics of the controller, the frequency components of the closed-loop response are calculated and inverse Fourier transformed to obtain the time response of the closed-loop system. Based on this idea, we propose here a method to calculate the time response of the feedback system when a controller to be evaluated is introduced, using only one-shot experimental data. Here, the time response calculated by this method is referred to as 'virtual time response'.

It is assumed that the controlled object $G(z)$ is a linear time-invariant discrete-time single-input single-output system, and one-shot experimental data is a time series $u_0(k)$, $y_0(k)$ of input/output of $G(z)$, where, z is a shift operator, $k(=1,\ 2,\dots,\ N)$ is the number of samples, and N is the total number of the data. $u_0(k)$ and $y_0(k)$ may be either a closed-loop response or an open-loop response. For notation purposes, the dependence on z and k will be omitted and will be reiterated when deemed necessary. Let r, d and d_u be the reference input, output disturbance and input disturbance to the closed-loop system to be evaluated respectively. Let discrete Fourier transforms of u_0, y_0, r, d and d_u be $u_0(j\omega)$, $y_0(j\omega)$, $r(j\omega)$, $d(j\omega)$ and $d_u(j\omega)$, respectively, where j is an imaginary unit, and ω [rad/s] is an angular frequency given by the following equation with a sampling time t_s [s].

$$\omega = 0,\ \frac{2\pi}{Nt_s},\ 2\frac{2\pi}{Nt_s},\ 3\frac{2\pi}{Nt_s},\ \cdots,\ (N-1)\frac{2\pi}{Nt_s} \qquad (1)$$

It is assumed that u_0, r, d, d_u and a linear time-invariant discrete-time controller K satisfies:

A1) u_0, r, d, and d_u are time series of integer periods of the periodic signal. It will be mentioned later that A1 is weakened to A6.

A2) u_0 includes frequency components of which frequencies are the same as the frequencies of components included in r, d, or d_u. In other words, if any of $r(j\omega_a)$, $d(j\omega_a)$, and $d_u(j\omega_a)$ is not 0 at a certain ω_a, then $u_0(j\omega_a) \neq 0$. Taking that contraposition, if $u_0(j\omega_a) = 0$ at a certain ω_a, then $r(j\omega_a) = d(j\omega_a) = d_u(j\omega_a) = 0$.

A3) K stabilizes the feedback system.

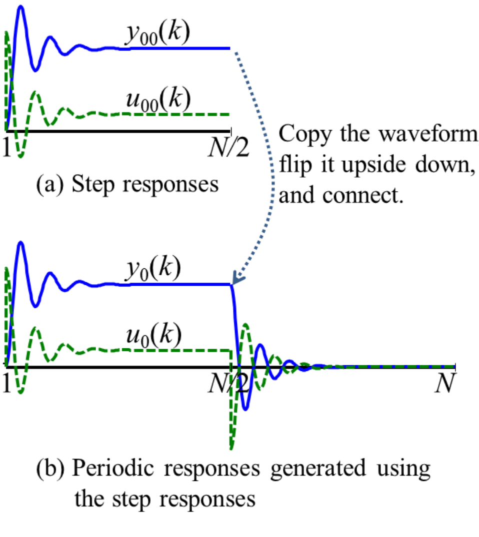

Fig. 1. Generating periodic responses using step responses: (a) Step responses $u_{00}(k)$ and $y_{00}(k)$. (b) Periodic responses $u_0(k)$ and $y_0(k)$ generated using $u_{00}(k)$ and $y_{00}(k)$, respectively.

A4) K^{-1} does not have the stability boundary pole. In other words, $K(j\omega) \neq 0$ at all ω. The optimization in Section 2.2 forces to satisfy A4 with constraint conditions.

A5) If G^{-1} has the stability boundary pole, K does not have the pole. In other words, if $G(j\omega_a) = 0$ at a certain ω_a, $K^{-1}(j\omega_a) \neq 0$. Taking that contraposition, if $K^{-1}(j\omega_a) = 0$ at a certain ω_a, then $G(j\omega_a) \neq 0$.

A procedure for creating a periodic signal that satisfies the assumption A1 is described using step response data u_{00} or y_{00} that satisfies the following assumption A6, see [Maeda (2019)].

A6) The initial value and the final value of the step response data u_{00} can be regarded as the steady state. This applies to y_{00} as well.

The open loop or closed-loop step responses u_{00} and y_{00} do not satisfy the assumption A1. However, after the step response waveform of Fig. 1a is copied, flipped upside down and connected, the waveform of Fig. 1b is derived which satisfies the assumption A1. Therefore, u_0 and y_0 are created by the following equations using step responses u_{00} and y_{00}.

$$u_0(k) = \begin{cases} u_{00}(k), \quad k = 1, 2, \cdots, \dfrac{N}{2} \\ -u_{00}\left(k - \dfrac{N}{2}\right) + u_{00}(1) + u_{00}\left(\dfrac{N}{2}\right), \\ \qquad k = \dfrac{N}{2} + 1, \dfrac{N}{2} + 2, \cdots, N \end{cases} \quad (2)$$

$$y_0(k) = \begin{cases} y_{00}(k), \quad k = 1, 2, \cdots, \dfrac{N}{2} \\ -y_{00}\left(k - \dfrac{N}{2}\right) + y_{00}(1) + y_{00}\left(\dfrac{N}{2}\right), \\ \qquad k = \dfrac{N}{2} + 1, \dfrac{N}{2} + 2, \cdots, N \end{cases} \quad (3)$$

If this procedure is applied to the step response u_{00} and y_{00} in Fig. 1a, u_0 and y_0 shown in Fig. 1b become one cycle of periodic signals and satisfy the assumption A1. Under the assumption A6, u_0 and y_0 correspond precisely to the true input and output responses of G. Since the periodic signal can be represented by the sum of sine waves, u_0, y_0, r, d, and d_u can be represented by the sum of sine waves according to the assumption A1. Then, since the frequency response is a steady-state characteristic and does not include a transient characteristic, let the discrete-time frequency transfer function of G and K be $G(j\omega)$ and $K(j\omega)$, respectively, it holds

$$y_0(j\omega) = G(j\omega)\, u_0(j\omega). \quad (4)$$

The equation (4) can be expressed as block diagram in Fig. 2a. Fig. 2b shows a block diagram of the feedback system when a controller $K(j\omega)$ whose control performance is to be evaluated is introduced. The calculation procedure of the time response y, u used to evaluate the performance of the control system in Fig. 2b is described from now. From Fig. 2b, it holds

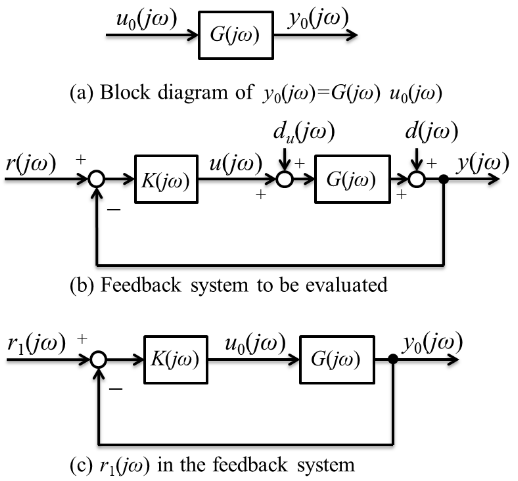

(a) Block diagram of $y_0(j\omega)$=$G(j\omega)$ $u_0(j\omega)$

(b) Feedback system to be evaluated

(c) $r_1(j\omega)$ in the feedback system

Fig. 2. Block diagram of: (a) $y_0(j\omega) = G(j\omega)u_0(j\omega)$. (b) Feedback system to be evaluated. (c) $r_1(j\omega)$ satisfies $y_0(j\omega) = G(j\omega)u_0(j\omega)$ in the feedback system.

$$\begin{aligned} y(j\omega) = & \frac{G(j\omega)\, K(j\omega)}{1 + G(j\omega)\, K(j\omega)} r(j\omega) \\ & + \frac{1}{1 + G(j\omega)\, K(j\omega)} d(j\omega) \\ & + \frac{G(j\omega)}{1 + G(j\omega)\, K(j\omega)} d_u(j\omega). \end{aligned} \quad (5)$$

Substituting (4) to this and multiplying the numerator/denominator by $K^{-1}(j\omega)u_0(j\omega)$, it holds

$$\begin{aligned} y(j\omega) = & \frac{y_0(j\omega)}{K^{-1}(j\omega)\, u_0(j\omega) + y_0(j\omega)} r(j\omega) \\ & + \frac{K^{-1}(j\omega)\, u_0(j\omega)}{K^{-1}(j\omega)\, u_0(j\omega) + y_0(j\omega)} d(j\omega) \\ & + \frac{K^{-1}(j\omega)\, y_0(j\omega)}{\underbrace{K^{-1}(j\omega)\, u_0(j\omega) + y_0(j\omega)}_{r_1(j\omega)}} d_u(j\omega). \end{aligned} \quad (6)$$

Let $r_1(j\omega)$

$$r_1(j\omega) = K^{-1}(j\omega)\, u_0(j\omega) + y_0(j\omega). \quad (7)$$

Substituting (7) into (6), the calculation formula of $y(j\omega)$ is obtained as

$$\begin{aligned} y(j\omega) = & \frac{r(j\omega)}{r_1(j\omega)} y_0(j\omega) \\ & + \frac{d(j\omega)}{r_1(j\omega)} K^{-1}(j\omega)\, u_0(j\omega) \\ & + \frac{d_u(j\omega)}{r_1(j\omega)} K^{-1}(j\omega)\, y_0(j\omega). \end{aligned} \quad (8)$$

$u(j\omega)$ can be calculated from Fig. 2b by the following formula:

$$u(j\omega) = K(j\omega)\, (r(j\omega) - y(j\omega)). \quad (9)$$

Block diagram in Fig. 2c is derived from (4) and (7). From Fig. 2c, r_1 is the reference input to the feedback system when the input and output response of G becomes u_0

and y_0 (in this case, $d = d_u = 0$). From (7), r_1 becomes bounded periodic signal under A1 and A4.

When $r_1(j\omega_a) = 0$ at a certain angular frequency ω_a, zero division occurs in (8), but, from now, it is shown that in that case there is no problem by setting $y(j\omega_a) = u(j\omega_a) = 0$. Because it holds $r_1(j\omega_a) = 0$ in Fig. 2c, the following equations are obtained for $y_0(j\omega_a)$ and $u_0(j\omega_a)$:

$$y_0(j\omega_a) = \frac{G(j\omega_a)K(j\omega_a)}{1 + G(j\omega_a)K(j\omega_a)} r_1(j\omega_a)$$

$$\therefore y_0(j\omega_a) = \frac{1}{\frac{1}{G(j\omega_a)K(j\omega_a)} + 1} 0 \tag{10}$$

$$u_0(j\omega_a) = \frac{K(j\omega_a)}{1 + G(j\omega_a)K(j\omega_a)} r_1(j\omega_a)$$

$$\therefore u_0(j\omega_a) = \frac{1}{K^{-1}(j\omega_a) + G(j\omega_a)} 0. \tag{11}$$

From (10), if $\frac{1}{G(j\omega_a)K(j\omega_a)} + 1 \neq 0$, it holds $y_0(j\omega_a) = 0$. From the Nyquist stability criterion, it holds $G(j\omega_a)K(j\omega_a) = -1$ only when the stability margin is zero, but this is not the case because the feedback system is stable under A3. Therefore, it holds $y_0(j\omega_a) = 0$. From (11), if $K^{-1}(j\omega_a) + G(j\omega_a) \neq 0$, it holds $u_0(j\omega_a) = 0$. It holds $K^{-1}(j\omega_a) + G(j\omega_a) = 0$ only when $G(j\omega_a)K(j\omega_a) = -1$ or $K^{-1}(j\omega_a) = G(j\omega_a) = 0$. From A3, it holds $G(j\omega_a)K(j\omega_a) \neq -1$. From A5, it holds $K^{-1}(j\omega_a) \neq 0$ when $G(j\omega_a) = 0$. So, it holds $u_0(j\omega_a) = 0$. Therefore, from A2, it holds $r(j\omega_a) = d(j\omega_a) = d_u(j\omega_a) = 0$. When $r(j\omega_a) = d(j\omega_a) = d_u(j\omega_a) = 0$, a similar argument is made for Fig. 2b from now. From (5), we get

$$\begin{aligned} y(j\omega_a) = &\frac{1}{\frac{1}{G(j\omega_a)K(j\omega_a)} + 1} 0 \\ &+ \frac{1}{1 + G(j\omega_a)K(j\omega_a)} 0 \\ &+ \frac{1}{G^{-1}(j\omega_a) + K(j\omega_a)} 0. \end{aligned} \tag{12}$$

Under A3, the first and second terms become zero. The third term becomes zero if $G^{-1}(j\omega_a) + K(j\omega_a) \neq 0$. It holds $G^{-1}(j\omega_a) + K(j\omega_a) = 0$ only when $G(j\omega_a)K(j\omega_a) = -1$ or $G^{-1}(j\omega_a) = K(j\omega_a) = 0$. From A3, it holds $G(j\omega_a)K(j\omega_a) \neq -1$, and from A4, it holds $K(j\omega_a) \neq 0$. So, the third term also becomes zero. Therefore, we get $y(j\omega_a) = 0$. Substituting this $y(j\omega_a) = 0$ and $r(j\omega_a) = 0$ into (9), we get $u(j\omega_a) = K(j\omega_a) \cdot 0$. Then we get $u(j\omega_a) = 0$ when $K^{-1}(j\omega_a) \neq 0$. When $K^{-1}(j\omega_a) = 0$, we get $G(j\omega_a) \neq 0$ under the contraposition of A5. Therefore, we get $u(j\omega_a) = 0$ by substituting $y(j\omega_a) = 0$ into $y(j\omega_a) = G(j\omega_a)u(j\omega_a)$. From the above, when $r_1(j\omega_a) = 0$ at a certain angular frequency ω_a, zero division occurs in (8), but it has been shown that in that case there is no problem by setting $y(j\omega_a) = u(j\omega_a) = 0$ instead of calculating (8) and (9). Under A1, A3, and A4, we get the time responses y and u those are the inverse discrete Fourier transformation of $y(j\omega)$ and $u(j\omega)$.

2.2 Virtual Time-response based Iterative Gain Evaluation and Redesign (V-Tiger)

Since this method is based on the Fourier transform of a periodic signal, it uses the characteristic of $G(j\omega)$ ignoring the real part of the pole of $G(s)$. Therefore, when the feedback system becomes unstable without satisfying the assumption A3, there is a problem that unstable transient characteristics cannot be reproduced. In order to solve this problem, we propose to avoid instability of the system by considering the stability margin.

From here, we describe the procedure for measuring the overshoot and settling time from the virtual time response, obtaining the stability margin from the input and output frequency components and $K(j\omega)$, and repeating the evaluation and redesign of the controller K. Let θ the adjustment parameter vector of the controller, and the discretized controller is represented by $K(\theta)$. For example, in the case of PID controller, we set $K(s) = K_p + \frac{K_i}{s} + K_d s$ where $\theta = (K_p \;\; K_i \;\; K_d)$. The discretized $K(\theta)$ is optimized using the following procedure:

1) Set the range of θ to be searched, and the allowable values for overshoot and stability margin.
2) Solve the constrained optimization problem to find $K(\theta)$ in which the objective function is settling time, and the constraint conditions are values of overshoot and stability margin. At this time, the overshoot and settling time are obtained from the virtual time response of the feedback system when using a controller derived by discretizing $K(\theta)$. The stability margin is obtained using the frequency characteristics of $G(j\omega) = \frac{y_0(j\omega)}{u_0(j\omega)}$ and $K(\theta)$. If G is unstable, the stability is checked using the Nyquist stability criterion. In addition, it is also a constraint that $K^{-1}(\theta)$ is stable so that assumption A4 is satisfied.

This procedure avoids destabilization of the system by considering the stability margin. Therefore, the problem that the error between the virtual time response and the true response diverges when $K(\theta)$ destabilizes the system is avoided. In this procedure, since the optimization is performed using the discretized $K(\theta)$, the influence of the discretization error of the controller has been considered. In numerical simulations and actual machine experiments described later, particle swarm optimization in [Chen (2009) and Perez (2007)] are used as a solver for the nonlinear optimization problem with constraints.

3. SIMULATION

The following nine continuous-time transfer functions give the same PID gain by the Ziegler-Nichols ultimate sensitivity method, see [Suda (1992)].

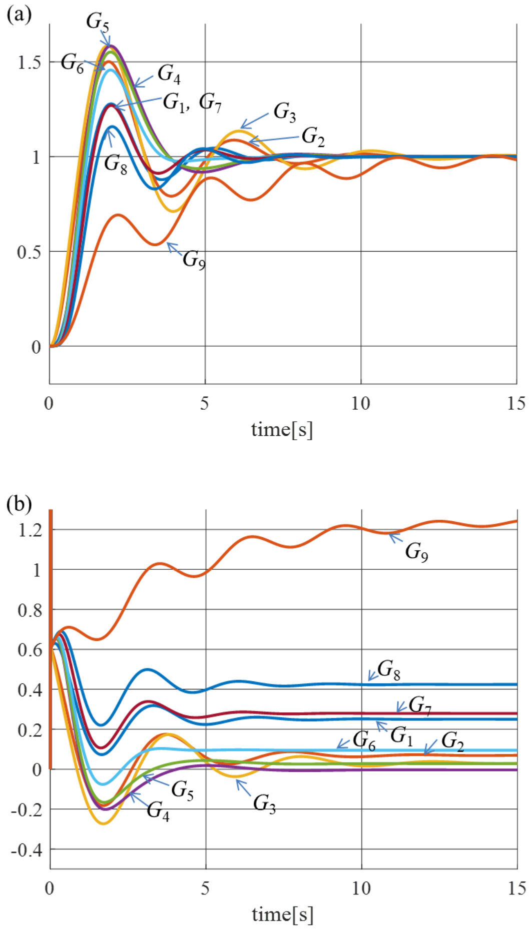

Fig. 3. Step responses when $G_1 \sim G_9$ were controlled using K designed by Ziegler-Nichols ultimate sensitivity method: (a) The output responses y_{00}. (b) The input responses u_{00}.

$$G_1(s) = \frac{64}{(s+2)^4} \tag{13}$$

$$G_2(s) = \frac{519.84}{(7s+18)(s+1)(5s+2)} \tag{14}$$

$$G_3(s) = \frac{130(3s+2)}{(s+1)(5s+2)(4s+1)(s+4)} \tag{15}$$

$$G_4(s) = \frac{2.57}{s(1+0.1625s)^5} \tag{16}$$

$$G_5(s) = \frac{44.45}{(1+17.12s)(1+0.1657s)^5} \tag{17}$$

$$G_6(s) = \frac{10.422}{(1+3.848s)(1+0.17687s)^5} \tag{18}$$

$$G_7(s) = \frac{3.625}{(1+1.0925s)(1+0.2114s)^5} \tag{19}$$

$$G_8(s) = \frac{2.4}{(1+0.3735s)(1+0.27315s)^5} \tag{20}$$

$$G_9(s) = \frac{12.8}{(s+2)^2(s^2+0.8s+4)} \tag{21}$$

The PID controller common to $G_1(s) \sim G_9(s)$ is

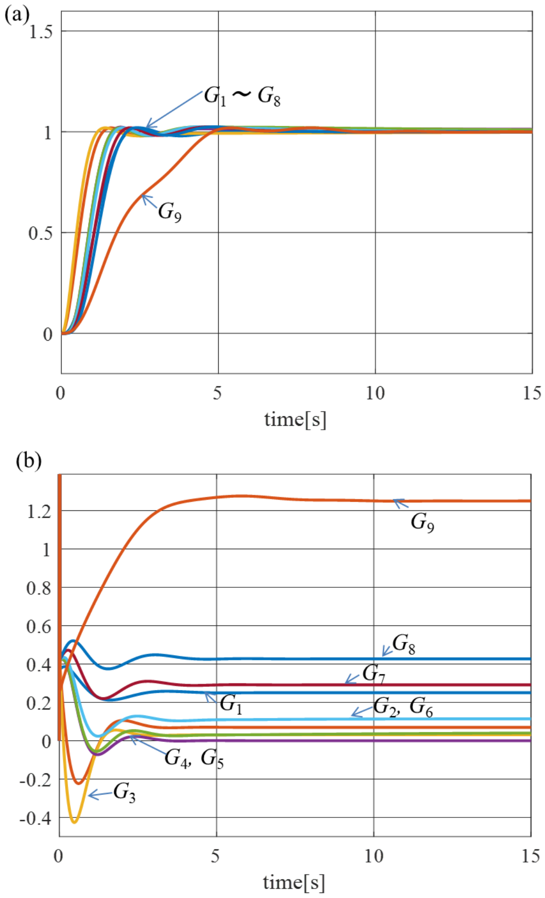

Fig. 4. Step responses when $G_1 \sim G_9$ were controlled using K designed by proposed V-Tiger method: (a) The output responses y. (b) The input responses u.

$$K(s) = 0.6\left(1 + \frac{1}{1.5708s} + 0.3927s\right). \tag{22}$$

The sample time t_s was 0.01s. Control objects $G_1(s)$ to $G_9(s)$ were Z-transformed with t_s. A controller K was discretized by substituting

$$s = \frac{1 - z^{-1}}{t_s} \tag{23}$$

into (22). y_{00} and u_{00} were respectively the input and output responses for 100s when the step function was input as the reference signal r. y_{00} and u_{00} from 0 to 15s were shown in Fig. 3. The responses after 15s were almost constant.

The constraint conditions were overshoot 3% or less, gain margin 3dB or more, and phase margin 20deg or more. The objective function was settling time within 2% of the steady value. For each of $G_1 \sim G_9$, the nonlinear optimization problem with constraints was solved for discretized $K(\theta)$ derived by substituting (23) into

$$K(s) = K_p + \frac{K_i}{s} + K_d s. \tag{24}$$

The particle swarm optimization 'pso' in [Chen (2009) and Perez (2007)] in MATLAB was used. The adjustment parameter vector was $\theta = (K_p \quad K_i \quad K_d)$, and the search range was from 0 to twice the PID gains in (22). In order

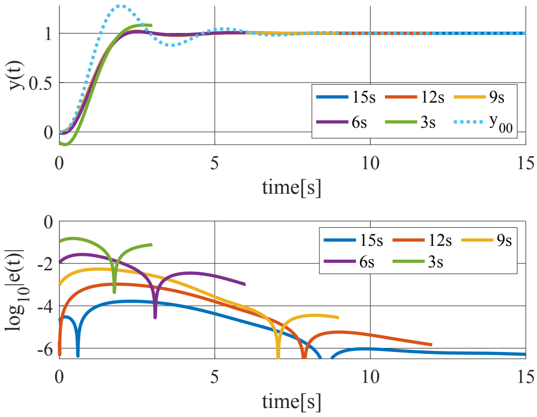

Fig. 5. The relationship between the time-length of y_{00} period (15s, 12s, 9s, 6s, and 3s) and the virtual time response error e for G_1: (a) Virtual time responses y versus time-length of y_{00}. (b) Virtual time responses error e versus time-length of y_{00}.

to satisfy the assumption A4, the constraint that the zero of $K(\theta)$ was stable and its real part size was 0.001 [rad/s] or more was added. Fig. 4 showed the true time responses of the feedback system when $K(\theta)$ obtained by the optimization was used. From Fig. 4, the overshoots were suppressed and the settling time was shortened in all of G_1 to G_9.

For G1, the relationship between the time-length of y_{00} period (15s, 12s, 9s, 6s, and 3s) and the virtual time response error e was shown in Fig. 5. The longer the time-length of y_{00} period, the smaller the error. This property was consistent with A6.

4. ACTUAL MACHINE EXPERIMENT

This method was applied to a real machine to verify its practicality. In order to remove the influence of noise, the Time-synchronous signal average was used in which the same waveform was acquired many times and takes an average. The actual machine used here was the DC motor. This DC motor (Bringsmart JGA25-371-463) had a gear head with a gear reduction ratio of 1: 21.3 and a rotary encoder with 12 counts per motor rotation. The rotary encoder output pulse signal was frequency-voltage converted by a FV converter (JRC NJM4151), and quantized by a 12-bit AD converter in a microcomputer Arduino DUE. The sample time was 0.01 s. The control input u calculated by the controller was limited to the power supply output range 0-5 V, quantized with 8 bit, converted to PWM with chopping frequency 1 kHz, and output to the motor driver (TA7291P) .

In this experiment, at first, the PID controller was designed using the Ziegler-Nichols ultimate sensitivity method, see [Suda (1992)], and the input/output responses were measured for 5 seconds when the reference speed was changed from 20 to 30 rpm. In order to prevent the control input to be saturated, filter for the reference signal $\frac{0.1}{1-0.9z^{-1}}$ was introduced so that the control input was within the range of 0-5V, and the dulled output of this filter was used as a reference input r. The measurement was repeated 50 times, and the noise was decayed by the Time-synchronous signal average by adding all waveforms and dividing by 50 to obtain u_{00} and y_{00}. The yellow lines in Fig. 6 showed u_{00} and y_{00} waveforms from 0 to 1[s].

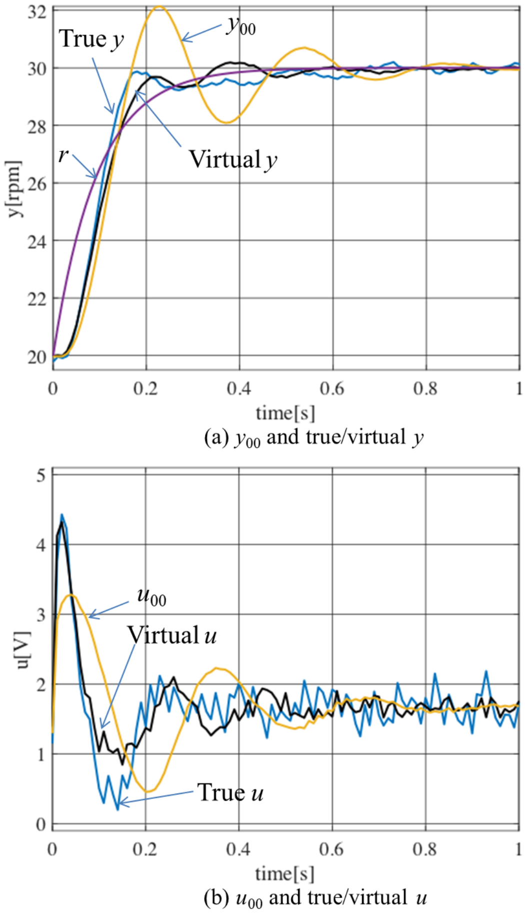

(a) y_{00} and true/virtual y

(b) u_{00} and true/virtual u

Fig. 6. y_{00}, u_{00}, and true/virtual time responses y, u using K designed by proposed V-Tiger method: (a) y_{00} and y. (b) u_{00} and u.

The constraint conditions were overshoot 3% or less, gain margin 3dB or more, and phase margin 20deg or more. The objective function was settling time within 2% of the steady value. The nonlinear optimization problem with constraints was solved for discretized $K(\theta)$ derived by substituting (23) into

$$K(s) = K_p + \frac{K_i}{s} + K_d s. \tag{25}$$

The particle swarm optimization ‘pso’ in [Chen (2009) and Perez (2007)] in MATLAB was used. The adjustment parameter vector was $\theta = (K_p \quad K_i \quad K_d)$, and the search range was from 0 to twice the PID gains used to measure y_{00}. Fig. 6 showed the true time responses (Blue lines) and virtual time responses (Black lines) of the feedback system when $K(\theta)$ obtained by the optimization was used. From Fig. 6, compared to y_{00}, the virtual time response and the true response had smaller overshoot and settling time. It was confirmed that the control performance was improved by our method. Fig. 6b showed a high initial actuation. Countermeasures against non-linearities including actuation saturation were future works.

5. CONCLUSION

Simulations and actual machine experiments confirmed that the control performance was improved by our method. Future work should focus on noise countermeasures when only a short-time response can be obtained, and analysis and countermeasures for the effects of nonlinearity including actuation saturation.

REFERENCES

Silver, D. et al. (2017). Mastering the game of Go without human knowledge. *Nature*, 550, 354–359.

Mnih, V. et al. (2015). Human-level control through deep reinforcement learning. *Nature*, 518, 529–541.

Surma, G. (2017). https://github.com/gsurma/ cartpole.

MATLAB pidtune. (2010). https:// www. mathworks.com/help/control/ref/pidtune.html.

Sample, I. (2017). 'It's able to create knowledge itself': Google unveils AI that learns on its own. *The Guardian.*

Kosaka, M. et al. (2020). Virtual Time-response based Iterative Gain Evaluation and Redesign (in Japanese). *T. of SICE*, 56(4).

Takahashi, H., Kaneko, O. (2019). A New Approach to Prediction of Responses in Closed Loop Systems Based on the Direct Usage of One-shot Experimental Data (in Japanese). *T. of SICE*, 55(4), 324–330.

Campi, M.C., Lecchini, A., Savaresi, S.M. (2002). Virtual reference feedback tuning: a direct method for the design of feedback controllers. *Automatica*, 38, 1337–1346.

Souma, S., Kaneko, O., and Fujii, T. (2004). A newmethod of controller parameter tuning based on input-output data, -Fictitious Reference Iterative Tunining. In *ALCOSP 04*, 789–794. IFAC.

Hoogendijk, R., Molengraft, M.J.G., Hamer, A.J., Steinbuch, M. (2015). Computation of transfer function data from frequency response data with application to data-based root-locus. *Control Engineering Practice*, 37, 20–31.

Karimi, A., Nicoletti, A., Zhu, Y. (2015). Robust H_∞ Controller Design Using Frequency-Domain Data via Convex Optimization. *Int. J. Robust. Nonlinear Control*, 28(12), 1–19.

Tasaka, K., Kano, M., Ogawa, M., Masuda, S., Yamamoto, T., (2009). Direct PID Tuning from Closed-Loop Data and Its Application to Unstable Processes (in Japanese). *T. of ISCIE*, 22(4), 137–144.

Takiyama, T., Yoshikawa, T., Noh, J., Ohta, Y. (2018). PI and Adaptive Model Matching Control System that Satisfies the Setting Settling Time, application to engine speed control. *IFAC Papers OnLine*, 51(4), 394–399.

Tachibana, H., Tanaka, N., Maeda, Y., Iwasaki, M. (2019) Comparisons of Frequency Response Function Identification Methods using Single Motion Data. In *ICM2019*, 498-503. IEEE.

Chen, S. (2009). Constrained Particle Swarm Optimization, https://www.mathworks.com/ matlabcentral/fileexchange/25986.

Perez, R. E., Behdinan, K. (2007). Particle swarm approach for structural design optimization. *Computers and Structures* 85, 1579-1588.

Suda, N., (1992). Systems, control and information library 6 PID Control (in Japanese), *Asakura*, 17–22